land

MDPI

Article

Low-Carbon Cropland Use Performance in China: Network Evolution, Structural Positions, and Governance Implications

Qi Xia, Yi Chen and Yinrong Chen *

College of Public Administration, Huazhong Agricultural University, Wuhan 430070, China; xiaqi0301@gmail.com (Q.X.); chy9647@163.com (Y.C.)
* Correspondence: cyr@mail.hzau.edu.cn

Abstract

Improving cropland carbon performance while maintaining food security is central to China's agricultural transition and climate goals This study examines low-carbon cropland use performance (PCLU) and its model-implied interprovincial association network across 31 Chinese provinces from 2010 to 2023. A global super-efficiency slacks-based measure model estimated PCLU by incorporating agricultural output, carbon emissions, nonpoint-source pollution, and crop sequestration; annual directed networks were constructed with a modified gravity model and analyzed using social network analysis, a temporal exponential random graph model (TERGM), and complementary quadratic-assignment analyses. Mean PCLU increased from 0.524 to 0.861, while the interquartile range widened from 0.146 to 0.310; network density declined before partially recovering as hierarchy increased, indicating improvement without provincial convergence and reconnection within a more differentiated multi-hub structure. Persistence (β = 4.510) and reciprocity (β = 2.376) dominated network evolution, whereas shared partners produced neither additional triadic closure nor expanding open chains; similarities in urbanization and planting structure favored ties, while rural-income differences reflected socioeconomic complementarity. External validation showed moderate overall correspondence with green-technology patent collaboration (mean annual QAP r = 0.335) but limited overlap among the strongest dyads. Overall, China's low-carbon cropland transition combined rising but increasingly uneven performance with a path-dependent and selective interprovincial structure, providing an empirical basis for differentiated coordination based on provincial performance and network position.

Keywords: low-carbon cropland use; land-use performance; model-implied spatial association network; temporal exponential random graph model; land governance

Check for updates

Academic Editor: Eduardo Gomes

Received: 14 July 2026
Revised: 9 August 2026
Accepted: 12 August 2026
Published: 17 August 2026

Copyright: © 2026 by the authors. Licensee MDPI, Basel, Switzerland. This article is an open access article distributed under the terms and conditions of the Creative Commons Attribution (CC BY) license.

1. Introduction

Agricultural land systems must increasingly secure food supplies while reducing emissions and maintaining ecological functions. These outcomes depend on interactions among biophysical conditions, production systems, institutions, markets, and cross-scale processes rather than on isolated local decisions [1–6]. Cropland is central to this challenge. Agricultural inputs and field operations generate carbon emissions, while crop growth and soil–plant processes contribute to carbon sequestration [7–9]. A low-carbon transition in cropland use must therefore be considered alongside food security, climate adaptation, and land degradation. Otherwise, mitigation pursued without a system-wide perspective may create trade-offs with food production, land demand, or other environmental

 https://doi.org/10.3390/land15081491

objectives [10–17]. This tension is especially important in China, where carbon-neutrality goals coexist with strict cropland-protection and grain-security priorities.

Existing research has approached this challenge from both performance-measurement and relational perspectives. Efficiency studies have progressed from single indicators to data envelopment analysis, slacks-based measure (SBM) models, global productivity indices, and super-efficiency models that jointly consider multiple inputs, desirable outputs, and undesirable outputs [18–21]. Applications to low-carbon cropland use performance (PCLU), cultivated-land eco-efficiency, and agricultural eco-efficiency have identified substantial regional differences associated with urbanization, resource endowments, production structure, and agricultural modernization [20–25]. Land-system, sustainability-transition, and network-governance research further emphasizes the importance of cross-scale interdependence and institutional coordination in sustainability transitions [26–30]. More directly, efficiency studies have already extended beyond province-by-province comparisons to spatial association networks. At national and subnational scales, networks have been constructed for agricultural carbon-emission efficiency, cultivated-land-use ecological efficiency, agricultural water-use efficiency, low-carbon agricultural total factor productivity, and agricultural green total factor productivity [31–37]. Using modified gravity models or VAR–Granger tests together with social network analysis, these studies have identified non-adjacent associations, central and peripheral nodes, and differentiated block structures.

These studies have substantially advanced efficiency research by treating relational structure as an object of analysis. However, most construct annual networks and then describe changes in density, centrality, and block structure. Their driving factors are commonly examined through QAP regressions based on representative-year or averaged matrices [31–37]. Such approaches reveal network patterns and the regional attributes associated with ties, but they do not jointly estimate temporal dependence and endogenous network configurations, including tie persistence, reciprocity, and shared partners. Dynamic generative models have only recently been introduced into efficiency-network research. Xu et al. applied a stochastic actor-oriented model (SAOM) to China's provincial agricultural water-use efficiency network [38], while Zhang et al. used a temporal exponential random graph model (TERGM) to examine urban land-use efficiency within the Yangtze River Delta [39]. The remaining gap is therefore not the absence of a network perspective, but its limited longitudinal application to nationwide low-carbon cropland use. In particular, little is known about how persistence, endogenous configurations, and provincial differences jointly shape a national PCLU network that incorporates agricultural production, carbon emissions, nonpoint-source pollution, and crop carbon sequestration. In this study, a tie represents a potential association generated by the gravity model from the PCLU levels and agricultural scales of two provinces under economic–geographic friction.

Cross-sectional quadratic assignment procedures can account for the dependence among matrix observations, but they cannot directly represent tie persistence, reciprocity, or shared-partner configurations. TERGMs address this limitation by modeling the network at each discrete observation point as a probability distribution conditional on previous networks and jointly estimating endogenous structural effects and time-varying covariates [40,41]. Alternative dynamic network models embody different assumptions about how ties change. Separable temporal exponential random graph models (STERGMs) distinguish tie formation from tie dissolution [42]; SAOMs represent network evolution as a sequence of actor-initiated micro-adjustments [43]; relational event models require time-stamped interaction-event data [44]; and dynamic latent-space models primarily characterize changes in unobserved node positions or group structures [45]. In this study, the annual interprovincial networks are reconstructed consistently from provincial attributes at

discrete time points rather than derived from continuous actor decisions or time-stamped interaction events. The discrete-time, whole-network framework of the TERGM is therefore better aligned with the structure of the data and the objective of examining temporal network dependence [46,47].

Against this background, this study examines PCLU and its model-implied interprovincial association network across 31 Chinese provinces from 2010 to 2023. It addresses three questions: (1) How did PCLU change under the joint demands of food security and carbon mitigation? (2) How did the network evolve, and which groups of provinces occupied net-spillover, broker, bidirectional-spillover, or net-beneficiary structural blocks? (3) How were tie persistence, reciprocity, shared partners, and non-geographic provincial differences conditionally associated with tie formation? We first estimate PCLU using a global super-efficiency SBM model and then employ a modified gravity model to construct annual directed networks. Social network analysis is used to describe network topology and provincial structural positions. A TERGM evaluates longitudinal dependence and endogenous network configurations, while distance-excluded MRQAP models provide complementary cross-sectional checks for selected years. External validity is assessed by comparing the symmetrized gravity network with observed interprovincial green-technology patent collaboration.

This study extends existing research in three respects. First, it constructs a nationwide cropland-performance network that incorporates carbon emissions and crop carbon sequestration. Second, it advances the analysis from descriptive network mapping to the longitudinal modeling of network persistence and endogenous dependence. Third, it identifies provincial structural positions and provides partial external validation against observed interprovincial green-technology patent collaboration while maintaining a clear distinction between model-implied associations and verified cooperation.

2. Materials and Methods

2.1. Study Area

The study covers 31 provincial-level administrative units in mainland China from 2010 to 2023 (Figure 1). Hong Kong, Macao, and Taiwan are shown for cartographic completeness but excluded from the analysis because of differences in statistical systems and data availability. The study area is divided into seven broad agricultural regions with substantial variation in climate, topography, water availability, and cropland endowment. Agricultural systems range from large-scale mechanized grain production in Northeast China and irrigated wheat-maize rotations in the Huang-Huai-Hai region to rice-based intensive cultivation in the middle and lower Yangtze region and South China. Mountainous and fragmented cropland characterizes Southwest China, irrigation is essential in the arid Northwest, and the Qinghai–Tibet Plateau has a short growing season and limited cropland. Figure 1 summarizes these differences and identifies the 13 major grain-producing provinces.

These regional contrasts affect PCLU through differences in production scale, cropping intensity, irrigation dependence, mechanization, and material inputs, which shape agricultural output, carbon emissions, nonpoint-source pollution, and crop carbon sequestration. They also provide the basis for selecting the provincial characteristics examined in the network analysis, including cropland endowment, irrigation, planting structure, multiple cropping, rural income, and urbanization. The provincial scale offers consistent statistical and policy units for national comparison, although it cannot capture heterogeneity within provinces.

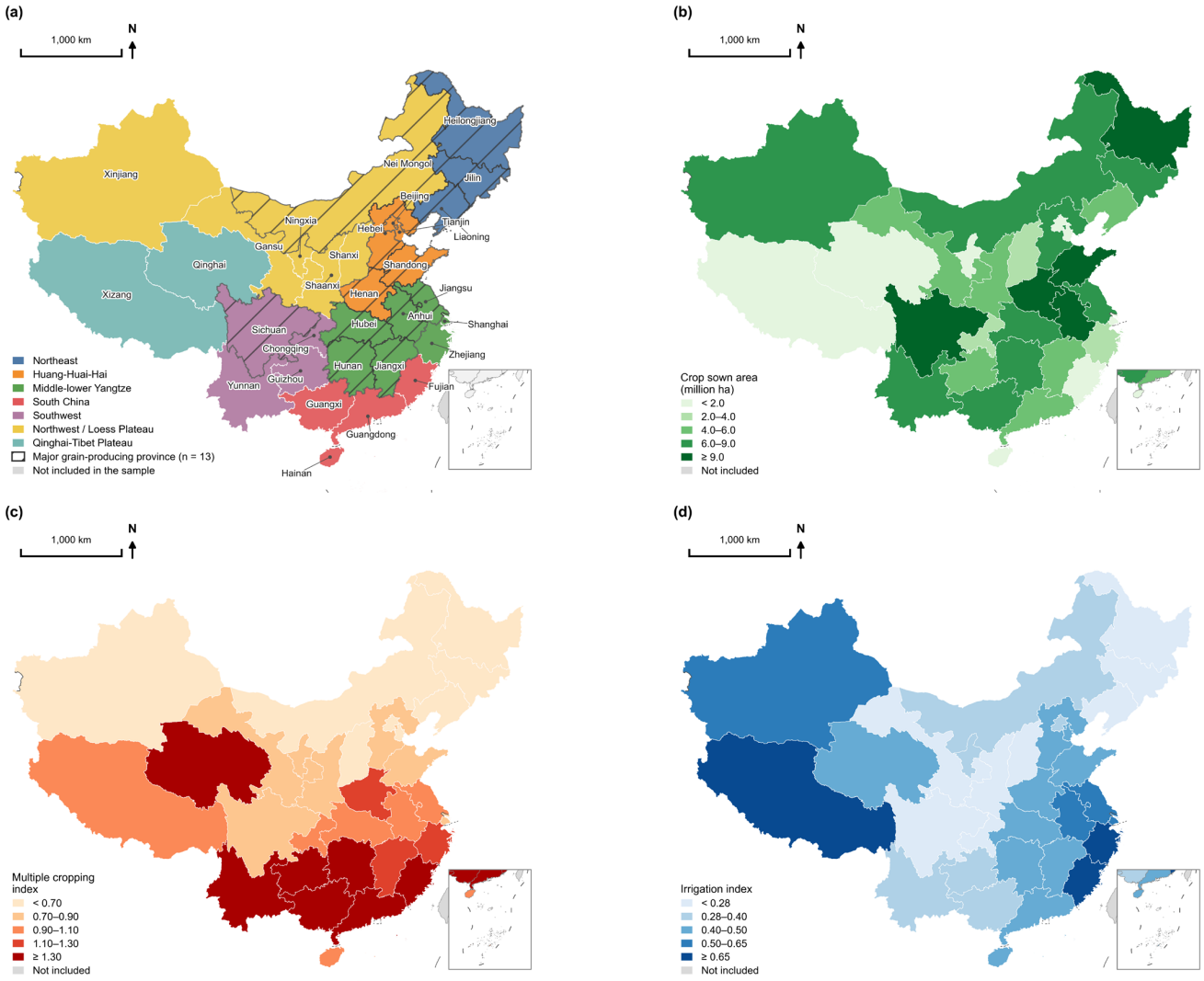


Figure 1. Study area and agricultural context. (**a**) Seven agricultural regions and 31 provincial-level units; hatching marks the 13 major grain-producing provinces. (**b**) Crop-sown area, (**c**) multiple-cropping index, and (**d**) irrigation index in 2023. Hong Kong, Macao, and Taiwan are displayed for cartographic completeness but excluded from the analysis. Base map: Tianditu (GS(2024)0650); projection: WGS 1984 UTM Zone 49N. Values above 1 in (**c**) and (**d**) reflect differences between activity and cropland-area statistics.

2.2. Data Sources

The period 2010–2023 captures sustained changes in cropland use and China's recent shift toward low-carbon agriculture. We compiled socioeconomic, agricultural production, resource input, and energy consumption data from national and provincial statistical yearbooks and provincial statistical bulletins. The variables shown in Figure 1 come from the same sources: crop-sown area and effective irrigated area from agricultural statistics, and cropland area from the national land survey. Administrative boundaries came from the National Platform for Common Geospatial Information Services (Tianditu; Map Review Number GS(2024)0650). Monetary variables used to measure performance were converted to constant 2010 prices where applicable. For external validation, we used annual province-pair data from the China National Intellectual Property Administration (CNIPA), reporting counts of jointly applied green-technology patents from 2010 to 2023. The data distinguish total applications, invention patents, and utility-model applications.

The analysis proceeds in five steps. First, we estimate agricultural carbon emissions and crop carbon sequestration for the environmental component of the indicator system.

Second, a global super-efficiency SBM model measures PCLU while accounting for undesirable outputs. Third, a modified gravity model converts provincial scores into annual directed networks. Fourth, social network analysis describes network structure and structural positions, and TERGM and MRQAP models assess the conditions associated with modeled tie formation. Fifth, observed interprovincial green-technology patent collaboration is used to evaluate the convergent validity of the model-implied network.

2.3. Indicator System

2.3.1. Input-Output Indicators for PCLU Measurement

PCLU measures how effectively a region produces agricultural value, grain, and crop carbon sequestration while limiting resource use and environmental pressure. The model includes land, labor, and material inputs; desirable economic, social, and environmental outputs; and two undesirable outputs, carbon emissions and nonpoint-source pollution. Following earlier work on cropland efficiency and agricultural carbon accounting [48], Table 1 organizes the indicators into these three groups. This structure allows the SBM model to treat environmental pressure as a by-product of production rather than as a separate descriptive measure.

Table 1. Input–output indicator system for measuring low-carbon cropland use performance.

Primary Indicator.	Secondary Indicator	Variable and Description	Abbreviation
Production input	Land	Crop-sown area (10^3 ha)	X1
	Labor	Agricultural labor: employment in agriculture, forestry, animal husbandry, and fishery × agriculture's share of total output from these sectors (10,000 persons)	X2
	Material input	Fertilizer application, pure amount (10,000 t)	X3
	Material input	Agricultural plastic film use (t)	X4
	Material input	Effective irrigated area (10^3 ha)	X5
	Material input	Total power of agricultural machinery (10,000 kW)	X6
Desirable output	Economic output	Total agricultural output value, deflated to 2010 constant prices (100 million yuan)	Y1
	Social output	Total grain output (10,000 t)	Y2
	Environmental output	Carbon sequestration from cropland (10,000 t)	Y3
Undesirable output	Carbon-emission output	Total carbon emissions from cropland use (10,000 t)	Z1
	Pollutant output	Total losses of fertilizer nitrogen/phosphorus, pesticides, and agricultural plastic film (10,000 t)	Z2

Land input is measured by crop-sown area. We estimate labor input by multiplying employment in agriculture, forestry, animal husbandry, and fishery by agriculture's share of their combined output. Material inputs include machinery power, fertilizer, effective

irrigated area, and agricultural plastic film. Desirable outputs are total agricultural output value, grain output, and estimated crop carbon sequestration. Undesirable outputs are agricultural carbon emissions and estimated losses of fertilizer, pesticides, and plastic film.

2.3.2. Factors Associated with Network Formation

We examine six provincial characteristics that may be related to the modeled PCLU ties (Table 2). Per capita cropland and the irrigation index represent the agricultural resource base. Planting structure and multiple cropping describe how cropland is used. Rural income and urbanization capture socioeconomic differences that may covary with technology-adoption capacity, service availability, and governance conditions. Each variable is converted into an annual matrix of absolute differences between provinces. Geographic distance is not included as an explanatory variable because the modified gravity model already uses economic–geographic distance to construct the network. Including it again would blur the distinction between constructing and explaining the dependent network.

Table 2. Non-geographic dyadic variables used in the TERGM and complementary MRQAP analyses.

Dimension	Indicator	Variable and Description	Code
Resource endowment	Per capita cropland	Cropland area/rural population	Z
Production conditions	Irrigation index	Effective irrigated area/cropland area	P
Production conditions	Planting structure	Grain sown area/total crop sown area	S
Production conditions	Multiple-cropping index	Crop sown area/cropland area	L
Socioeconomic conditions	Rural income	Natural logarithm of rural per capita disposable income	E
Socioeconomic conditions	Urbanization	Urban population/total population	U

2.4. Research Methods

2.4.1. Carbon Emission and Sequestration Measurement

Cropland use both emits and removes carbon. Fertilizer, pesticides, agricultural plastic film, diesel, irrigation, and tillage generate emissions, whereas crop growth and biomass accumulation sequester carbon. Following established agricultural carbon-accounting methods [7,8], we calculate emissions and sequestration for each province as follows:

$$C_{ei} = \sum P_j \cdot \delta_j \quad (1)$$

$$C_{si} = \sum \frac{Y_c \cdot \delta_c \cdot (1 - W_c)}{H_c} \quad (2)$$

In Equations (1) and (2), CE_i is total carbon emissions in province i (t). P_j is the amount or activity level of source j, and delta_j is its emission coefficient. The sources include fertilizer, pesticides, agricultural plastic film, diesel, irrigation, and tillage. CS_i is total crop carbon sequestration in province i (t). For crop c, Y_c is economic yield, delta_c is the carbon absorption rate, W_c is moisture content, and H_c is the economic coefficient. Table 3 reports the crop-specific parameters.

Table 3. Parameters for estimating carbon sequestration of major crops.

Crop	Economic Coefficient (H^c)	Moisture Content (%)	Carbon Absorption Rate (δ^c)
Rice	0.45	12	0.414
Wheat	0.40	12	0.485
Maize	0.40	13	0.471

Table 3. *Cont.*

Crop	Economic Coefficient (H^c)	Moisture Content (%)	Carbon Absorption Rate (δ^c)
Millet	0.42	12	0.450
Sorghum	0.35	12	0.450
Beans (total)	0.34	13	0.450
Tubers	0.70	70	0.423
Peanut	0.43	10	0.450
Rapeseed	0.25	10	0.450
Sunflower seed	0.30	10	0.450
Cotton	0.10	8	0.450
Sugarcane	0.50	50	0.450
Sugar beet	0.70	75	0.407
Tobacco	0.55	85	0.450
Vegetables	0.60	90	0.450

2.4.2. Global Super-Efficiency SBM Model

We estimate PCLU with a super-efficiency slacks-based measure (SBM) model [18,49,50]. The model accounts for non-radial input and output slacks, includes undesirable outputs, and ranks efficient decision-making units (DMUs). To make scores comparable over time, we pool all province-year observations in a single global production frontier [19]. Under constant returns to scale, PCLU for province k in year t is defined as follows:

$$\rho_k^{G,t} = \min \frac{1 + \frac{1}{m}\sum_{i=1}^{m} \frac{s_{ik}^t}{x_{ik}^t}}{1 - \frac{1}{s_1 + s_2}\left(\sum_{r=1}^{s_1} \frac{s_{rk}^{d,t}}{y_{rk}^{d,t}} + \sum_{q=1}^{s_2} \frac{s_{qk}^{b,t}}{y_{qk}^{b,t}}\right)} \tag{3}$$

$$\text{s.t} \begin{cases} x_k^t - \sum\limits_{j=1, j\neq k}^{N} \text{if } \tau = t \sum\limits_{\tau=1}^{T} \lambda_j^\tau x_j^\tau + s_k^t \geq 0 \\ \sum\limits_{j=1, j\neq k}^{N} \text{if } \tau = t \sum\limits_{\tau=1}^{T} \lambda_j^\tau y_j^{g,\tau} - y_k^{g,t} + s_k^{g,t} \geq 0 \\ y_k^{b,t} - \sum\limits_{j=1, j\neq k}^{N} \text{if } \tau = t \sum\limits_{\tau=1}^{T} \lambda_j^\tau y_j^{b,\tau} + s_k^{b,t} \geq 0 \\ 1 - \frac{1}{s_1 + s_2}\left(\sum\limits_{r=1}^{s_1} \frac{x_{rk}^{d,t}}{y_{rk}^{d,t}} + \sum\limits_{q=1}^{s_2} \frac{s_{qk}^{b,t}}{y_{qk}^{b,t}}\right) \geq \varepsilon \\ \lambda_j^\tau \geq 0, s_k^t \geq 0, s_k^{g,t} \geq 0, s_k^{b,t} \geq 0 \end{cases} \tag{4}$$

In Equations (3) and (4), rho_{kt}^{GSE} is the global super-efficiency PCLU score for province k in year t. The vectors x, y^g, and y^b denote inputs, desirable outputs, and undesirable outputs; s^−, s^+, and s^{b−} are their slack vectors. The intensity vector lambda_{j tau} places province-year observations on the global production frontier. The evaluated observation (k,t) is excluded from its own reference set so that efficient DMUs can be ranked.

2.4.3. Modified Gravity Model

We use a modified gravity model to translate provincial PCLU scores into potential interprovincial spatial associations [51,52]. Operationally, an association is the relative propensity for a province pair to be linked given their joint PCLU, agricultural scale, and economic–geographic friction. It is a model-implied proximity measure, not an observed record of cooperation, technology transfer, knowledge exchange, or policy coordination.

Gravity models represent interaction as increasing with the scale of the two regions and decreasing with distance [51,52]. Here, modeled association strength increases with agricultural scale and PCLU in both provinces and decreases with economic–geographic distance:

$$R_{ij} = K_{ij} \cdot \frac{\sqrt[3]{G_i P_i E_i} \cdot \sqrt[3]{G_j P_j E_j}}{D_{ij}^2} \quad (5)$$

$$K_{ij} = \frac{E_i}{E_i + E_j}, D_{ij}^2 = \left(\frac{d_{ij}}{g_i - g_j} \right)^2 \quad (6)$$

In Equations (5) and (6), R_ij is the directed model-implied association from province i to province j, and K_ij is the directional contribution coefficient. E_i and E_j are the two PCLU scores. G and P denote agricultural output value and the agricultural labor force. Economic–geographic distance D_ij combines the geodesic distance d_ij between provincial capitals with per capita agricultural output g. We convert the continuous matrix into a binary network using the mean of each row. A tie from i to j equals 1 when R_ij exceeds the mean association generated for province i, and 0 otherwise. This province-specific rule retains direction without imposing one national cutoff. It identifies associations that are strong relative to each sender's modeled profile.

2.4.4. Social Network Analysis (SNA)

In the PCLU network, provinces are nodes and directed model-implied associations are ties [53]. At the network level, density measures the share of possible modeled ties that are present. Hierarchy describes asymmetric dependence, and efficiency indicates how far the network avoids redundant connections. At the node level, normalized out-degree centrality measures the breadth of outgoing modeled ties, closeness centrality measures accessibility, and betweenness centrality identifies structural brokerage positions. We identify structurally similar groups with the CONCOR algorithm in UCINET, using a maximum split depth of 2 [54]. Following established block-modeling practice in spatial association network research [55,56], block roles are identified jointly from three indicators: the number of external outgoing ties, the number of external incoming ties, and the comparison between the actual and expected proportions of within-block ties. The combined relational profiles distinguish net-spillover, broker, bidirectional-spillover, and net-beneficiary blocks. These labels describe the relative structural functions of different blocks within the PCLU association network. The actual proportion is the number of within-block ties divided by all ties sent by that block. The expected proportion is $(n_k - 1)/(N - 1)$, where n_k is block size and N is the number of provinces.

2.4.5. Temporal Exponential Random Graph Model and Complementary MRQAP

The TERGM uses the 14 annual directed networks from 2010 to 2023 and models the network in year t conditional on the previous network and current dyadic covariates [41]. TERGM is selected because the estimand is a whole-network tie probability conditional on prior network structure. By contrast, SAOM assumes that actors make sequential micro-changes to their outgoing ties between observation waves [43], an actor-level choice process that is not observed for gravity-reconstructed provincial ties. MRQAP does not supply this longitudinal dependence model and is therefore retained only as a cross-sectional check. The TERGM specification includes edges, reciprocity, geometrically weighted edgewise shared partners (GWESP), geometrically weighted dyadwise shared partners (GWDSP), first-order tie persistence, and six time-varying covariates. GWESP and GWDSP use outgoing two-paths and a fixed decay of 0.5. GWESP captures closed outgoing two-paths among tied province pairs and therefore tests residual triadic closure, whereas GWDSP

captures shared outgoing partners across dyads and tests the prevalence of open shared-partner configurations. These terms distinguish baseline sparsity, reciprocal ties, closed and open shared-partner structures, and persistence. All coefficients are interpreted as conditional log-odds associations rather than causal effects.

$$Pr(Y_t = y_t | Y_{t-1}, X_t) \propto exp\left\{\theta^T s(y_t, Y_{t-1}, X_t)\right\} \quad (7)$$

In Equation (7), Y_t is the directed network in year t, X_t contains the six annual difference matrices, and s(·) contains the endogenous and exogenous network statistics. Each covariate is $|x_it - x_jt|$ and is standardized using the pooled off-diagonal mean and standard deviation across all years. Rural income is log-transformed before the difference is calculated. We estimate the model by bootstrapped maximum pseudolikelihood with 1000 replications. For each of the 13 annual transitions, 100 simulated networks are compared with the observed density, reciprocity, and mean number of outgoing two-path shared partners. We also estimate Double Dekker semi-partialling MRQAP models for 2010, 2015, 2020, and 2023 with 2000 permutations [57]. The directed network is symmetrized only for this cross-sectional analysis. Geographic distance is excluded from both sets of explanatory variables.

2.4.6. Robustness Checks

We use four checks to test whether the findings are sensitive to network construction, centrality measurement, temporal specification, or the provincial sample. First, we compare the row-mean threshold with a global mean and with rules that retain the strongest 30% and 20% of ties. We compare density, connectedness, hierarchy, efficiency, and overlap among leading nodes. Second, we retain the continuous gravity scores and compare binary total degree with weighted total strength using rank correlations and leading-node overlap.

Third, we compare several TERGM specifications: a temporal-covariate model, a reciprocity model, the selected GWESP-GWDSP model, and models with additional in-degree and out-degree heterogeneity. We evaluate them using the area under the receiver operating characteristic curve (AUC), average precision, Brier score, log loss, parsimony, and simulation-based fit. Fourth, we re-estimate the distance-excluded MRQAP models after removing Beijing, Tianjin, Shanghai, and Chongqing. We compare coefficient directions, permutation p values, and fit between the 31-province and 27-province samples. The Supplementary Materials provide the full results.

We prepared the networks, ran robustness checks, and produced figures in Python 3.12 with pandas, NumPy, SciPy, NetworkX, GeoPandas, and Matplotlib. TERGM and MRQAP models were estimated in R 4.4 with btergm and asnipe, respectively. Spatial figures use WGS 1984 UTM Zone 49N where appropriate. The Supplementary Materials retain processed matrices, scripts, bootstrap estimates, simulation summaries, and source data for the figures.

2.4.7. External Validation of the Model-Implied Network

Because the gravity network is model-implied rather than observed, we assessed its convergent validity against an independent province-pair record of interprovincial green-technology patent collaboration. The CNIPA dataset reports annual counts of jointly applied green-technology patents from 2010 to 2023 and distinguishes total applications, invention patents, and utility-model applications. Hong Kong, Macao, and Taiwan were excluded to match the 31-province sample, and diagonal values were set to zero. Because patent collaboration is symmetric, the annual gravity intensity was symmetrized as (Rij + Rji)/2. Total collaborative patent applications were used as the primary measure, and invention-patent collaboration provided a stricter robustness measure.

We used two complementary layers of validation. First, annual QAP Spearman correlations with 2000 node-label permutations assessed dyadic rank correspondence between the symmetrized gravity and patent-collaboration matrices [57,58]. We also calculated the Jaccard overlap of the top-decile ties, the area under the receiver operating characteristic curve (AUC) for distinguishing province pairs with and without patent collaboration, and the Spearman correlation between provincial gravity strength and total collaboration volume. Second, a double-semi-partialling MRQAP regressed log-transformed collaboration counts, log(1 + count), on the logged gravity matrix while controlling for agricultural scale and logged geographic distance, again using 2000 permutations [57]. This stricter test asks whether the gravity matrix corresponds to the observed collaboration beyond two major components embedded in its construction. These procedures test correspondence rather than equivalence: patent collaboration records green-innovation interaction and is not a direct measure of agricultural extension, technology transactions, or policy coordination.

3. Results

3.1. PCLU Measurement and Spatiotemporal Evolution

The global super-efficiency SBM results indicate that China's provincial PCLU remained below the efficiency frontier for most of the study period. The national mean was 0.633 during 2010–2023, suggesting substantial scope for improving the conversion of agricultural inputs into desirable outputs while reducing carbon emissions and other environmental pressures (Figure 2). Its temporal evolution can be divided into two stages. From 2010 to 2016, the mean increased moderately from 0.524 to 0.583, and provincial values remained concentrated at relatively low levels. This pattern indicates that low PCLU was a broadly shared constraint across provinces rather than a problem confined to a small number of lagging regions.

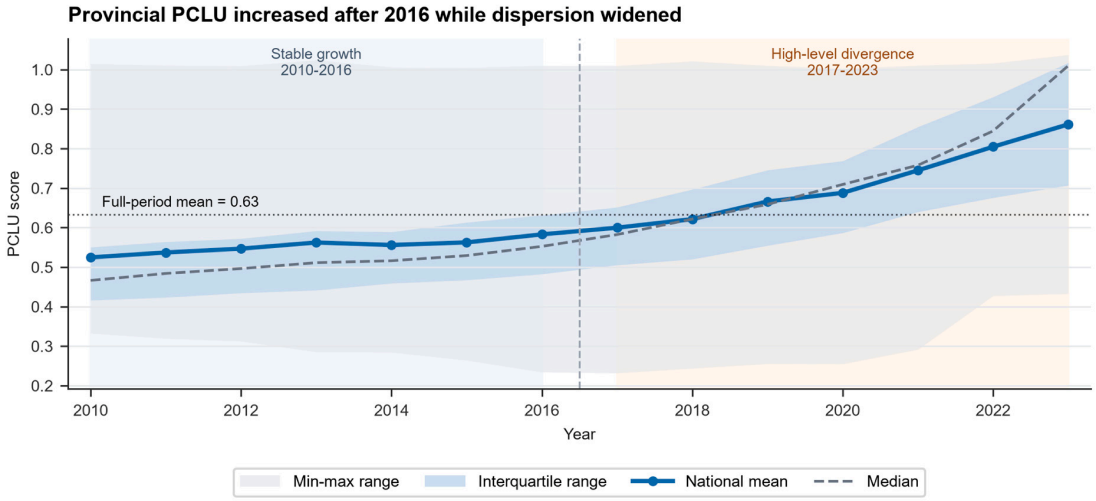


Figure 2. Annual trend and interprovincial dispersion of low-carbon cropland use performance in China, 2010–2023.

A more pronounced improvement occurred after 2017. The national mean rose from 0.600 in 2017 to 0.861 in 2023, accompanied by a rightward shift and flattening of the distribution (Figure 3). However, the interquartile range widened from 0.146 to 0.310. The later period was therefore characterized by an upward shift without corresponding convergence: more provinces moved toward higher PCLU levels, but the pace and extent of improvement became increasingly uneven. This divergence may reflect differences in agricultural modernization, production structure, resource constraints, and the capacity to reduce material inputs and environmental pressures while maintaining agricultural output.

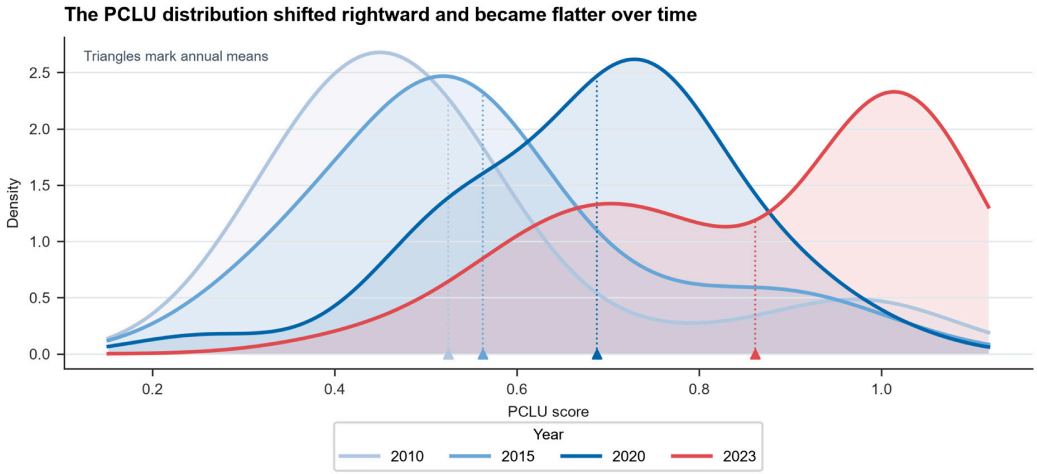


Figure 3. Kernel density distributions of low-carbon cropland use performance in selected years.

The spatial distribution further demonstrates that agricultural production scale does not directly translate into high PCLU (Figure 4). High-performing provinces were concentrated primarily in parts of Northwest and Northeast China, including Xinjiang, Qinghai, and Heilongjiang, whereas several major agricultural provinces in central and eastern China, such as Henan, Hebei, and Shandong, remained at medium or relatively low levels. This contrast reflects the multidimensional nature of PCLU: provinces are evaluated not only by agricultural output, but also by the balance among resource inputs, carbon emissions, pollution pressures, and carbon sequestration. Intensive grain-producing regions may consequently face greater difficulty in improving PCLU when output growth remains dependent on fertilizers, machinery, irrigation, and other carbon-intensive inputs.

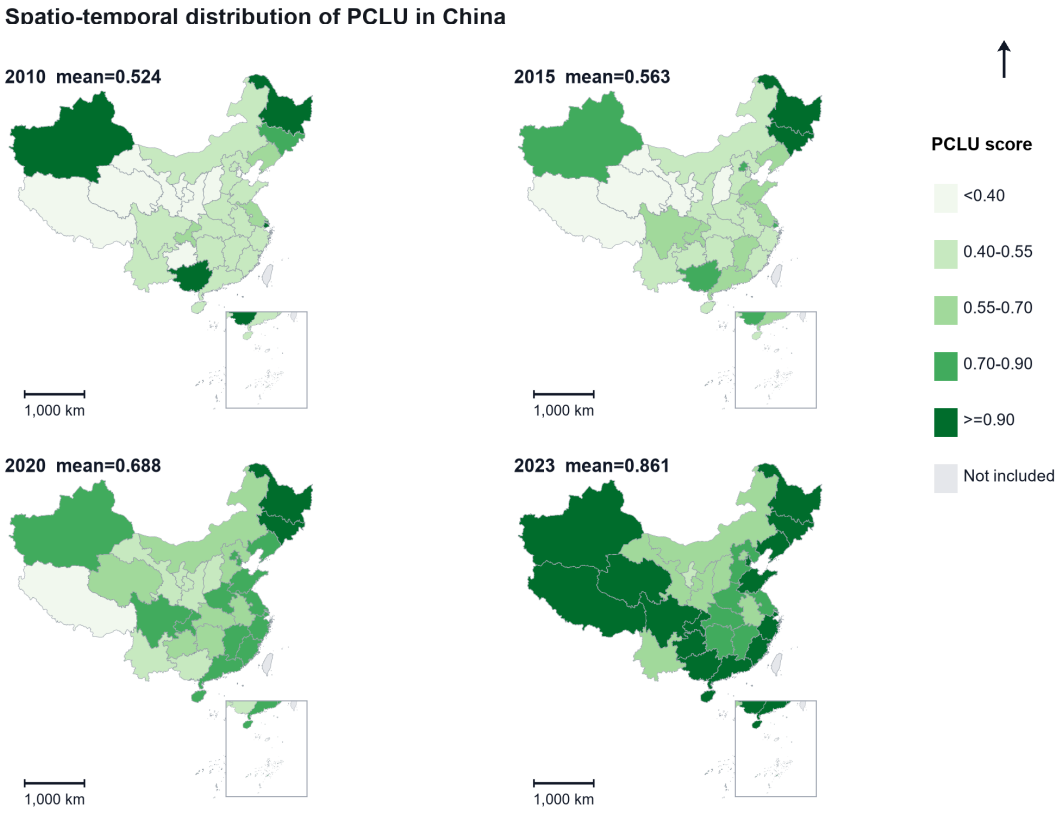


Figure 4. Spatiotemporal distribution of low-carbon cropland use performance in China, 2010–2023. Note: Class intervals are fixed across years.

Although the number of high-PCLU provinces increased and the spatial extent of low-performing areas contracted, relative disadvantages persisted in parts of central China. The results therefore reveal simultaneous national improvement and regional differentiation. This widening dispersion raises a further relational question: whether provinces with different PCLU levels remain broadly interconnected or become organized around increasingly selective ties and differentiated structural roles.

3.2. Spatial Association Network Analysis

The widening provincial dispersion in PCLU raises the question of how provinces with different performance levels are organized within the national network. This section examines the issue from three complementary dimensions: overall network evolution, changes in provincial centrality, and block-level structural differentiation.

3.2.1. Overall Network Structure and Evolution

The gravity model produced a fully connected yet increasingly selective national PCLU network (Figure 5). Connectedness remained 1.00 throughout 2010–2023, indicating that no province became isolated from the national association system. Network density nevertheless declined from 0.2935 in 2010, corresponding to 273 ties, to 0.2452 in 2017, corresponding to 228 ties, before recovering to 0.2720 in 2023, with 253 ties. The coexistence of complete reachability and declining density indicates selective contraction rather than network fragmentation: all provinces remained connected, but increasingly through fewer direct ties. Since density and tie count in 2023 remained below their 2010 levels, the post-2017 increase represents partial reconnection rather than continuous network expansion.

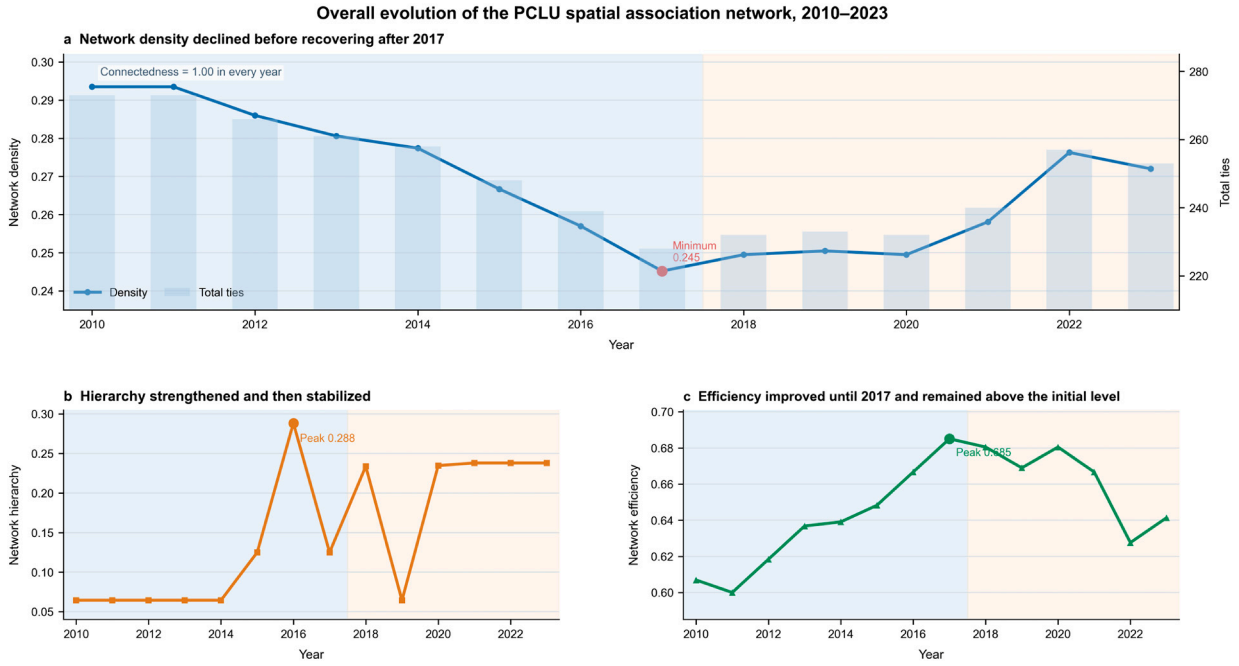


Figure 5. Evolution of overall indicators in the PCLU spatial association network, 2010–2023. Note: Density and total ties describe connection intensity; hierarchy and efficiency describe structural differentiation and redundancy reduction, respectively. Light background shading marks the density-contraction period (2010–2017) and the partial-reconnection period (2018–2023).

Network hierarchy increased from 0.0645 in 2010 to 0.2381 in 2023, with a pronounced peak in 2016. Meanwhile, network efficiency rose from 0.6069 in 2010 to 0.6851 in 2017 and subsequently declined to 0.6414 in 2023. These trends reveal a two-stage structural reorganization. During the contraction stage, fewer ties coincided with lower relational

redundancy and stronger hierarchical differentiation. Subsequent reconnection did not restore the earlier, more broadly distributed structure: hierarchy remained well above its initial level, while efficiency retained part of its earlier increase. The network therefore recovered within a more stratified architecture, with connectivity increasingly concentrated in selected provinces and interprovincial corridors.

3.2.2. Individual Node Centrality Analysis

Provincial positions within the network changed substantially between 2010 and 2023 (Table 4). Zhejiang and Fujian recorded the largest increases in both normalized out-degree and closeness centrality and ranked among the most central provinces in 2023. Shaanxi also experienced a marked increase, indicating the emergence of a stronger inland hub. In contrast, Shanghai, Beijing, and Liaoning showed pronounced declines in normalized out-degree or closeness centrality. These changes suggest that network advantages were progressively redistributed from several traditional eastern centers toward a broader set of coastal and inland provinces. Full province-level results are reported in Table S4.

Table 4. Summary of key node centrality changes in the PCLU spatial association network.

Metric	Leading Provinces in 2023	Largest Increases, 2010–2023	Largest Declines, 2010–2023	Interpretation
Normalized out-degree centrality (ODC)	Zhejiang (93.33); Fujian (83.33); Shaanxi (66.67); Shandong (60.00)	Zhejiang (50.00 to 93.33, +43.33); Fujian (50.00 to 83.33, +33.33); Shaanxi (43.33 to 66.67, +23.34)	Shanghai (83.33 to 16.67, −66.66); Beijing (46.67 to 13.33, −33.34); Liaoning (50.00 to 23.33, −26.67)	Connectivity breadth
Closeness centrality (CC)	Zhejiang (93.75); Fujian (85.71); Shaanxi (75.00); Shandong (71.43)	Zhejiang (66.67 to 93.75, +27.08); Fujian (65.22 to 85.71, +20.49); Shaanxi (62.50 to 75.00, +12.50)	Shanghai (85.71 to 54.55, −31.16); Jiangsu (81.08 to 69.77, −11.31); Liaoning (66.67 to 56.60, −10.07)	Network accessibility
Betweenness centrality (BC)	Tianjin (15.14); Fujian (12.65); Shaanxi (10.41); Shandong (7.40)	Tianjin (1.05 to 15.14, +14.09); Zhejiang (1.21 to 6.92, +5.71); Fujian (7.52 to 12.65, +5.13)	Hubei (9.04 to 1.24, −7.80); Liaoning (13.89 to 6.65, −7.24); Gansu (11.73 to 4.70, −7.03)	Brokerage/ intermediary position

Centrality is relational and therefore reflects a province's position relative to changes elsewhere in the network. The rise of Zhejiang and Fujian may be associated with the joint effects of their improving PCLU, agricultural scale, and favorable economic–geographic position within the gravity specification, which enabled them to establish associations with a wider range of provinces. Shaanxi's increasing centrality may additionally reflect its position between eastern, central, and western agricultural systems, allowing it to connect otherwise separated parts of the network. Conversely, the declining centrality of Beijing and Shanghai is consistent with the relative contraction of agriculture in highly urbanized economies, while Liaoning's decline may reflect slower relative improvement compared with the provinces whose network positions strengthened.

Betweenness centrality reveals a different dimension of structural influence. Tianjin, Fujian, and Shaanxi occupied prominent bridging positions in 2023, even though they did not always have the largest number of direct ties. Their importance therefore arose from connecting different parts of the network rather than simply accumulating relationships.

Taken together, the three centrality measures indicate that the network was not reorganized around a single dominant coastal core. Instead, it developed a multi-hub structure in which several provinces performed complementary functions as highly connected centers, inland junctions, or cross-regional intermediaries.

3.2.3. Block Modeling

Block modeling reveals relational differentiation without network fragmentation. CONCOR divided the 2023 network into four structurally equivalent blocks (Table 5), but only 54 of the 253 directed ties occurred within blocks, whereas 199 ties crossed block boundaries. The 78.7% interblock share indicates that national connectivity depended primarily on relationships among provinces occupying different structural positions. Block membership therefore does not represent geographically closed clusters. Instead, provinces are grouped according to similar patterns of sending and receiving ties, while the overall network is sustained by cross-block complementarity.

Table 5. Structural block roles and relation profiles in the model-implied PCLU association network in 2023.

Block	Structural Role	Provinces	External Outgoing/ Incoming Ties	Actual/Expected Internal-Tie Proportion	Main Linkage Pattern	Conditional Policy Implication
Block 1	Net-spillover role	Beijing; Shanghai; Xinjiang; Jilin; Inner Mongolia; Liaoning; Ningxia; Heilongjiang; Henan; Qinghai; Shandong	81/29	12.90%/33.33%	More outgoing than incoming external ties	Candidate hosts for demonstration platforms, subject to observed capacity and cooperation data.
Block 2	Broker role	Shanxi; Hebei; Tianjin; Gansu	20/34	28.57%/10.00%	Strong internal cohesion combined with cross-block relations	Candidate coordinators for paired extension teams and joint trials, subject to external validation.
Block 3	Bidirectional-spillover role	Anhui; Hunan; Hainan; Guangdong; Jiangsu; Hubei; Chongqing; Guangxi; Jiangxi	41/48	32.79%/26.67%	Outgoing and incoming external ties are broadly balanced	Candidate sites for reciprocal pilots and shared monitoring, subject to verification.
Block 4	Net-beneficiary role	Zhejiang; Yunnan; Shaanxi; Fujian; Tibet; Sichuan; Guizhou	57/88	19.72%/20.00%	More incoming than outgoing external ties	Candidate priorities for extension, finance, and locally adapted support, subject to needs assessment.

Note: External outgoing and incoming ties exclude within-block ties. The actual internal-tie proportion equals within-block ties divided by all outgoing ties from that block. The expected proportion is $(n_k - 1)/(N - 1)$. Role labels follow the joint pattern of outgoing and incoming ties and the actual and expected internal-tie proportions [55,56].

The four blocks performed distinct but interdependent structural functions. Block 1 was strongly outward-oriented, with 81 external outgoing ties and only 29 incoming ties, while its proportion of internal ties was substantially below the expected level. Its geographically dispersed provinces were therefore linked more strongly to other blocks than to one another. Block 2 combined an internal-tie proportion nearly three times its expected value with extensive cross-block connections, forming a relatively cohesive intermediary channel. Block 3 exhibited the most balanced external relations and above-expected internal cohesion, enabling it to connect with other blocks while maintaining a comparatively stable internal structure. Block 4 received substantially more external ties than it sent, while its internal concentration remained close to the expected level, indicating that its structural position was shaped primarily by extensive connections received from other blocks. Figure 6 visualizes these differentiated block roles within the weighted provincial network.

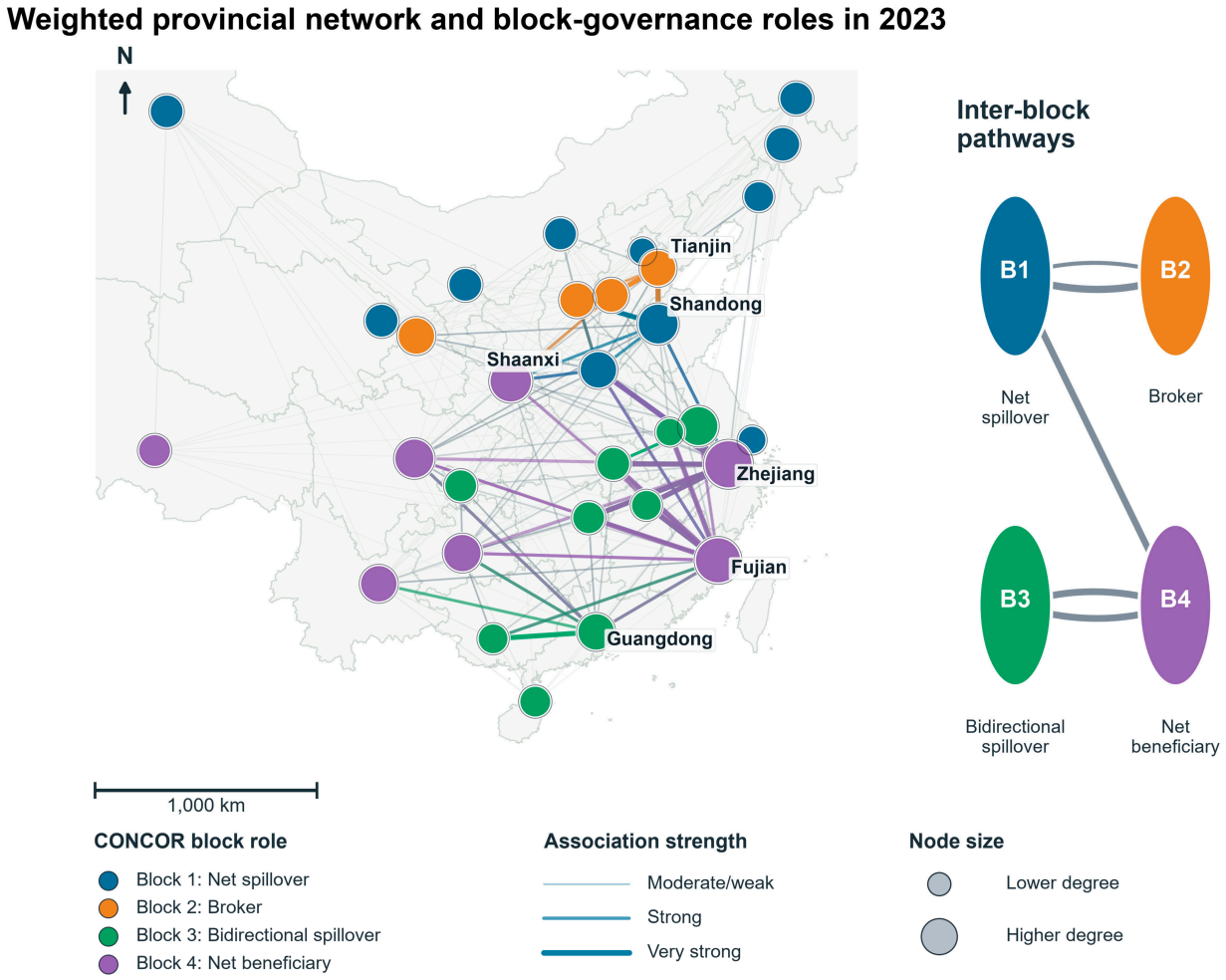


Figure 6. Weighted provincial PCLU association network and structural block roles in 2023.

These block roles do not constitute a ranking of provincial performance. Block 4, for example, included both highly connected provinces such as Fujian and Zhejiang and a weakly connected province such as Tibet. Its total degree ranged from 10 to 37, while PCLU ranged from 0.567 to 1.020. Such internal variation demonstrates that block roles describe the aggregate direction and concentration of relationships, whereas centrality and PCLU identify the structural position and performance of individual provinces. Read together, the results reveal a multi-layered and multi-hub national structure composed of

outward-oriented, cohesive-intermediary, reciprocally connected, and externally receptive blocks, rather than a simple coastal–inland or high–low performance hierarchy.

3.3. Factors Associated with Network Formation

3.3.1. Temporal Exponential Random Graph Model Results

The selected TERGM showed strong discriminatory performance (AUC = 0.977; average precision = 0.951; Brier score = 0.042) and reproduced most observed network statistics. Its central finding is pronounced temporal dependence. Tie persistence was the strongest structural effect (β = 4.510; odds ratio = 90.967), followed by reciprocity (β = 2.376; odds ratio = 10.761). Thus, current ties were strongly conditioned by both previous and reverse-direction ties. The persistence effect is consistent with gradual changes in PCLU and agricultural scale, while stable agricultural programs and production-service patterns provide plausible institutional context. Reciprocity indicates that a modeled tie was more likely when the reverse-direction tie was also present (Table 6 and Table S5; Figure S4).

Table 6. TERGM estimates for the PCLU spatial association network, 2010–2023.

Term	Estimate	95% Bootstrap CI	Odds Ratio	Interpretation
Edges (baseline)	−2.217	[−2.599, −1.907]	0.109	Supported; sparse baseline
Reciprocity	2.376	[1.939, 2.704]	10.761	Supported; reciprocal dependence
Closed two-paths (GWESP)	0.076	[−0.032, 0.152]	1.079	Not independently supported
Open/shared two-paths (GWDSP)	−0.393	[−0.444, −0.355]	0.675	Supported structural control
Tie persistence	4.510	[3.708, 5.533]	90.967	Supported; strong path dependence
Urbanization difference	−0.372	[−0.519, −0.260]	0.689	Supported; similarity association
Multiple-cropping difference	−0.088	[−0.162, 0.011]	0.916	Uncertain
Irrigation difference	0.209	[−0.038, 0.453]	1.232	Uncertain
Per capita cropland difference	0.008	[−0.114, 0.108]	1.008	Uncertain
Rural-income difference	0.294	[0.106, 0.465]	1.342	Supported; positive gradient
Planting-structure difference	−0.164	[−0.264, −0.068]	0.849	Supported; similarity association

Note: Coefficients are conditional log-odds estimates. Confidence intervals are based on 1000 bootstrap replications. Dyadic covariates are pooled-standardized absolute differences; supported terms have 95% intervals that exclude zero.

Higher-order network dependence was comparatively limited. GWESP was not independently supported (β = 0.076; 95% CI: −0.032 to 0.152), indicating no additional tendency toward triadic closure among provinces sharing outgoing partners. GWDSP was significantly negative (β = −0.393; odds ratio = 0.675), showing that open shared-partner configurations occurred less frequently after persistence, reciprocity, and other terms were controlled. Common partners therefore neither systematically closed triangles nor generated expanding open chains. This result indicates that the network was organized mainly around persistent reciprocal dyads and selected interprovincial corridors rather than generalized cluster-based expansion.

Different provincial characteristics displayed distinct association patterns. Urbanization and planting-structure differences were negatively associated with ties, suggesting that similar development stages and crop systems favored association. Rural-income difference was positively associated with ties, indicating socioeconomic complementarity between provinces at different income levels. Multiple cropping, irrigation, and per capita cropland were not independently supported. Network formation was therefore more consistently associated with relational history and production-system compatibility than with any single difference in agricultural resource endowment.

3.3.2. Complementary Distance-Excluded MRQAP Analysis

The MRQAP models explained 13.4–20.2% of matrix variation across the four representative years and revealed both recurrent and period-specific associations. Planting-structure and multiple-cropping differences were negative and statistically supported in every year, whereas per capita cropland difference remained unsupported. Urbanization difference became negative and supported in 2020 and 2023. Rural-income difference was positive in all four years and statistically supported from 2015 onward. Irrigation difference was supported only in 2020 and marginally supported in 2023, indicating a more period-specific relationship (Table 7; full estimates in Table S6).

Table 7. Standardized coefficients from the complementary distance-excluded MRQAP models.

Variable	2010	2015	2020	2023
Urbanization difference	0.136	−0.129	−0.283 ***	−0.285 ***
Multiple-cropping difference	−0.154 **	−0.163 ***	−0.219 ***	−0.183 ***
Irrigation difference	−0.044	−0.012	0.246 ***	0.142 *
Per capita cropland difference	−0.008	−0.056	−0.087	−0.014
Rural-income difference	0.131	0.237 ***	0.297 ***	0.255 **
Planting-structure difference	−0.133 **	−0.180 ***	−0.155 ***	−0.191 ***

Note: ***, **, and * denote permutation $p < 0.01$, $p < 0.05$, and $p < 0.10$, respectively. Each model uses 2000 Double Dekker semi-partialling permutations.

Comparison with the TERGM clarifies the temporal meaning of these results. The consistently negative planting-structure coefficient in both models indicates that production-system similarity characterized both annual network patterns and longitudinal tie formation. Multiple-cropping similarity was repeatedly observed in the cross-sectional models but was not independently supported by the TERGM, suggesting that its cross-sectional association was absorbed by network history and endogenous dependence. Urbanization and rural-income differences showed broadly consistent directions across the two approaches, whereas irrigation remained temporally unstable. Overall, persistence and reciprocity anchored network evolution, provincial characteristics influenced the selection of ties, and shared partners did not generate generalized clustering. Figure 7 summarizes the longitudinal and cross-sectional results.

3.4. Robustness Checks

The robustness checks test whether the main conclusions depend on the threshold used to create binary ties, the use of unweighted centrality, the TERGM specification, or the inclusion of municipalities. Table 8 summarizes the results, and the Supplementary Materials provide full estimates and simulation diagnostics.

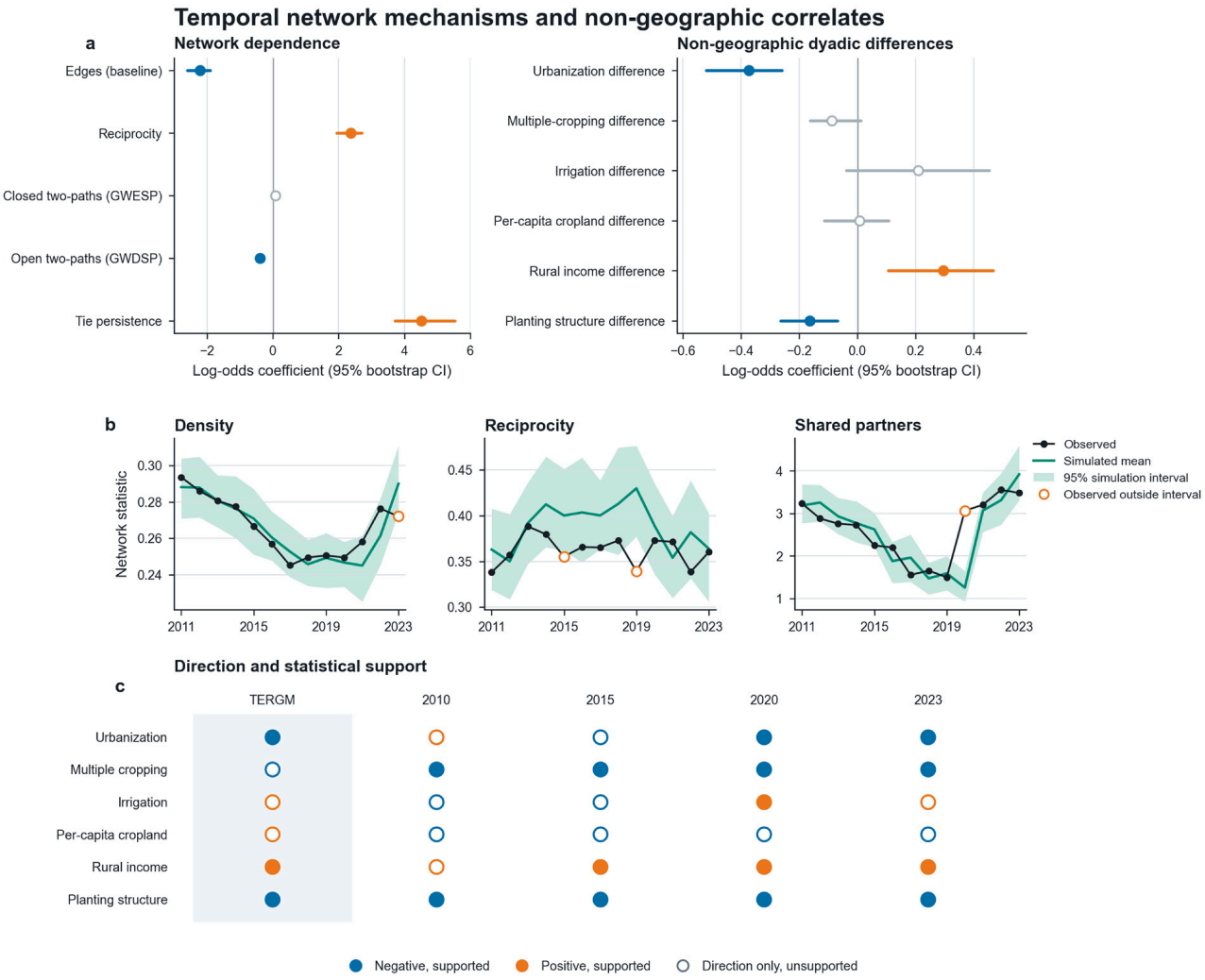


Figure 7. Temporal network mechanisms and non-geographic correlates of the provincial PCLU association network: (**a**) TERGM coefficient estimates and 95% bootstrap confidence intervals; (**b**) TERGM goodness-of-fit diagnostics for density, reciprocity, and shared-partner statistics; and (**c**) comparison of coefficient directions and statistical support between the TERGM and dis-tance-excluded MRQAP models for 2010, 2015, 2020, and 2023.

Table 8. Summary of robustness checks for the PCLU spatial association network.

Robustness Check	Design	Main Evidence	Interpretation
Alternative thresholds	Row-mean baseline compared with global-mean, top-30%, and top-20% rules.	Thresholds changed sparsity, but 2023 top-10 node overlap was 1.00 under all alternatives.	Core-node identification is not threshold-specific.
Weighted centrality	Binary total degree compared with weighted total strength.	Spearman correlation = 0.553–0.762 ($p < 0.01$); top-10 overlap = 0.60–0.80.	Hub structure persists when tie intensity is retained.
TERGM specification and goodness of fit	Alternative structural terms compared; 100 simulations per transition.	AUC improved from 0.960 to 0.977; density/shared partners covered in 12/13 years and reciprocity in 11/13.	Selected model balances predictive fit, structure, and parsimony.

Table 8. *Cont.*

Robustness Check	Design	Main Evidence	Interpretation
Distance-excluded MRQAP and municipality exclusion	Six-variable models for four years; four municipalities removed in the reduced sample.	Directions unchanged in 22/24 comparisons; R^2 = 0.134–0.202 (full) and 0.158–0.258 (reduced).	Main directions are broadly stable, but several year-specific associations are sample-sensitive.

Alternative thresholds changed the number of ties but not the identity of the leading nodes. The global-mean and top-share rules produced different levels of sparsity and connectedness, as expected. In 2023, however, all three alternative rules reproduced the baseline top 10 nodes. Across representative years, overlap generally ranged from 0.60 to 1.00. The leading-node pattern therefore did not depend on the row-mean threshold alone (Table S1; Figure S1).

The weighted analysis produced similar hub rankings when binary total degree was compared with weighted total strength. Spearman correlations ranged from 0.553 to 0.762 across 2010–2023 and were statistically significant in every year ($p < 0.01$); the two rankings shared 60–80% of their top 10 provinces. This check evaluates the stability of overall hub prominence rather than reproducing the normalized out-degree measure in Table 4 (Table S2; Figure S2).

The model comparisons favored the selected GWESP-GWDSP TERGM. Relative to the simpler GWESP model, its AUC rose from 0.960 to 0.977 and average precision from 0.927 to 0.951. It also used fewer structural terms than the full degree-heterogeneity model. In the final simulation test, the observed density and shared-partner statistic were covered in 12 of 13 years, and reciprocity in 11. The remaining departures were concentrated in specific years rather than spread throughout the study period (Table S5; Figure S4).

Removing the four municipalities preserved the coefficient direction in 22 of 24 variable-year comparisons. MRQAP R^2 ranged from 0.134 to 0.202 in the full sample and from 0.158 to 0.258 in the reduced sample; statistical support changed in five comparisons. The broad patterns for urbanization, production conditions, and rural income were therefore stable, although some year-specific estimates remained sensitive to the sample. Across all checks, the most consistent findings were tie persistence, reciprocity, leading-node stability, similarity in urbanization and planting structure, and a positive rural-income gradient (Tables S3 and S6; Figure S3).

3.5. External Validation

External validation proceeded in two stages. First, annual QAP rank correlations, dyad-classification AUC, node-level Spearman correlations, and top-decile overlap were used to assess the overall correspondence between gravity-based association intensity and observed green-technology patent collaboration. Second, MRQAP models treated patent collaboration as the dependent network and examined whether gravity intensity retained an association after controlling for agricultural scale and geographic distance. This design distinguishes broad network correspondence from the portion attributable to scale and geographic proximity.

The two networks showed moderate overall correspondence. Annual QAP correlations were positive and statistically supported in all 14 years, ranging from 0.257 to 0.436, with a mean of 0.335. The mean AUC was 0.703, and the mean node-level Spearman correlation was 0.470. Correspondence among the strongest dyads was weaker: the mean top-decile Jaccard coefficient was 0.108, equivalent to an average overlap of 19.3% relative to the gravity network's leading ties. The invention-patent measure produced a similar pattern, with a mean QAP correlation of 0.312, a mean AUC of 0.689, and a

mean node-level correlation of 0.465. Thus, the gravity network captured the broad distribution of interprovincial collaboration more effectively than the exact composition of its strongest ties.

After controlling for agricultural scale and distance, the gravity coefficient remained positive and statistically supported during 2010–2015 (0.116–0.146, $p < 0.01$), was borderline in 2016 (0.068, $p = 0.0505$), and was unsupported from 2017 onward. The invention-patent specification showed a broadly similar temporal pattern. Meanwhile, patent-network density increased from 0.477 to 0.931, and geographic distance remained negatively associated with collaboration throughout the study period. As patent collaboration became denser and more geographically structured, gravity intensity contributed less additional information beyond scale and proximity. Overall, the external validation supports the gravity network as an indicator of the broad opportunity structure for interprovincial association, while its correspondence with specific dyads remains partial (Figure S5).

4. Discussion

4.1. Temporal Evolution and Policy Implications

China's provincial PCLU improved, but this improvement did not produce convergence. After 2017, the national mean rose more rapidly while provincial dispersion widened, indicating that provinces differed increasingly in their capacity to combine agricultural output with lower resource use and environmental pressure. The spatial mismatch between agricultural production and PCLU reinforces this interpretation. Several major grain-producing provinces in central and eastern China remained at medium or relatively low levels, whereas parts of Northwest and Northeast China performed better. Because PCLU evaluates the balance among output, material inputs, pollution, carbon emissions, and crop sequestration, production scale alone cannot guarantee high performance. Intensive grain-producing regions face a particularly sharp challenge: maintaining food-security functions while reducing dependence on fertilizer, machinery, and irrigation. The national improvement is consistent with Wu et al. [20], while the lower mean in this study may reflect its longer period, global production frontier, and inclusion of non-CO_2 pollution.

The U-shaped density trajectory adds a relational dimension to this differentiated transition. Network contraction during 2010–2017 coincided with stronger policy emphasis on resource conservation, input reduction, pollution control, and production restructuring, a pattern consistent with a greater role for within-province adjustment during this period. Partial reconnection after 2018 accompanied the integration of rural revitalization, high-standard farmland construction, agricultural modernization, and low-carbon development. However, density remained below its initial level and hierarchy remained elevated, indicating that reconnection was concentrated in selected provinces and corridors. The policy objective should therefore not be to maximize the number of ties, but to maintain sufficient coordination while improving their relevance and durability. During contraction, common standards and capacity support can prevent weaker provinces from becoming marginalized; during recovery, verified partnerships and reciprocal pilots can be expanded between established hubs and provinces facing stronger food-security–mitigation trade-offs.

4.2. Network Structure and Spatial Governance

Rather than following a simple coastal–inland hierarchy, the network remained nationally connected while ties became concentrated around several regional hubs. Building on previous studies of agricultural carbon-efficiency networks [31,32], this study broadens the performance concept by incorporating agricultural output, carbon emissions, pollution, and crop sequestration, and further shows that overall connectedness can coexist with increasingly selective interprovincial ties. The consistency of the leading-node pattern across

alternative thresholds and weighted networks also indicates that the multi-hub structure is not specific to one method of network binarization. Provincial PCLU is therefore embedded in a relational system characterized by national connectedness and differentiated structural positions.

Block roles reflect this structural division rather than a ranking of provincial performance. Their pronounced internal heterogeneity supports a two-level governance approach: block profiles indicate appropriate forms of coordination, whereas PCLU, centrality, implementation capacity, and existing cooperation determine province-specific responsibilities. High-performing and strongly connected members of the net-spillover block could host demonstration programs. Tianjin could coordinate partner matching within the broker block, while Guangdong and Jiangsu could lead reciprocal trials. Within the net-beneficiary block, Fujian, Zhejiang, and Shaanxi could organize partnerships among members with weaker connectivity. This arrangement links collective block functions with the capacities of individual provinces.

Translating these roles into action requires a connected chain of responsibility. National agencies could establish monitoring, reporting, and verification standards, maintain a shared project database, and co-finance interprovincial pilots. Provincial agricultural departments could convert these standards into partner selection, matching funds, and implementation evaluation. Regional platforms led by broker provinces could coordinate extension teams and joint trials of machinery, crop varieties, and low-carbon practices. Local extension agencies, cooperatives, and service providers would then adapt these practices to local farming systems and report implementation outcomes.

Comparable patterns in other agricultural regions provide a broader context. Brokerage supports knowledge exchange within England's fragmented land-management advisory system [59]; local–provincial relationships support knowledge creation and sharing in Ontario [60]; and research and extension organizations occupy central positions in agricultural innovation networks in Central Africa [61]. These cases show that hubs and brokers are not unique to China, although their functions depend on the surrounding institutional system. China's network is distinguished by nationwide connectedness, strong temporal persistence, and substantial provincial diversity. For other large and heterogeneous countries, the implication is that national standards, regional brokerage, and local adaptation need to operate as an integrated governance system.

External validation helps define how this network can be used. The gravity and patent-collaboration networks corresponded at the overall and node levels, but only partly identified the same strongest dyads. After agricultural scale and distance were controlled, the additional correspondence was concentrated in the early study period and weakened as patent collaboration became denser. The gravity network is therefore most informative for comparing broad structures and screening potential partners. Decisions concerning specific provincial partnerships should additionally consider observed cooperation, implementation capacity, and local production conditions.

4.3. Factors Associated with Network Formation

The longitudinal analysis shifts the interpretation of network formation from static provincial attributes to a path-dependent process. This path dependence has both model-based and institutional foundations. Distance is stable, while agricultural scale and PCLU generally change gradually; multiyear programs and established production-service patterns may also contribute to continuity in provincial associations. Reciprocity adds a second layer of structural stability because a modeled tie is more likely when the reverse-direction tie is present. Persistent and reciprocal structures may concentrate association opportunities among established province pairs. Governance experiments should therefore test whether

stable association patterns can support durable coordination while creating entry points for less-connected provinces.

Partner selection combined similarity in production conditions with complementarity in socioeconomic capacity. Provinces with comparable urbanization levels and planting structures were more likely to be connected, suggesting that similar transition pressures and crop systems reduce coordination and adaptation costs. Rural-income differences, by contrast, were positively associated with ties, indicating potential complementarity between financial capacity, service supply, and local demand. The MRQAP results sharpen this interpretation: multiple-cropping similarity appeared consistently in annual networks but lost independent support after persistence and endogenous dependence were considered. A cross-sectional resemblance in resource use does not necessarily become a stable driver of network change. Partner selection should therefore combine production-system compatibility with complementary capacity and financing arrangements.

The shared-partner results reveal a predominantly dyadic rather than cluster-led organization. Common outgoing partners neither generated additional triadic closure nor accumulated into expanding open chains. A shared intermediary therefore did not automatically produce new ties between otherwise unconnected provinces. This helps explain why broad diffusion cannot be expected to emerge from existing hubs alone. Broker provinces and regional platforms need an explicit convening function, supported by partner-matching mechanisms, joint funding, and common evaluation. Direct bilateral agreements may stabilize priority relationships, while formally coordinated consortia can connect provinces across different blocks and development levels.

4.4. Limitations

External validation strengthens the empirical basis of the gravity network but covers only one dimension of interprovincial relations. Green-technology patents record research collaboration across broad technological fields rather than agriculture-specific extension, technology transactions, input flows, or policy learning. The observed correspondence therefore supports the broad network structure more strongly than the identification of particular dyads. Future validation should combine several relational indicators, including agricultural co-patents, technology-transfer contracts, machinery and seed transactions, intergovernmental agreements, and collaboration among extension organizations. Different indicators would validate distinct dimensions of interprovincial association rather than require one proxy to represent all forms of interaction.

The temporal model also involves simplifying assumptions. The TERGM assumes stable coefficients over the study period and uses bootstrapped maximum pseudolikelihood. Although it reproduced most network statistics, its weaker fit to the 2020 shared-partner structure suggests a possible temporal break. Period-specific TERGMs or separable models could distinguish changes in tie formation and dissolution around such periods. The binary network further removes variation in association intensity. The weighted robustness analysis supports the main hub pattern, but future valued-network models could examine whether tie strength follows the same temporal mechanisms.

Finally, the provincial scale provides consistent statistical and policy units but conceals variation in land quality, farm structure, and extension capacity. Nested province–prefecture comparisons or regional case studies would help determine how aggregation affects network structure, although nationally consistent subprovincial data on emissions, pollution, sequestration, and cooperation remain limited. The models identify conditional network relationships rather than policy effects. Their main practical value is therefore to identify candidate partnerships, coordination structures, and testable intervention designs.

Subsequent pilots and implementation evaluation are required to determine whether these arrangements improve low-carbon cropland use.

5. Conclusions

This study examines the evolution of PCLU and its interprovincial association network across China from 2010 to 2023. Four conclusions emerge.

(1) Provincial PCLU improved but did not converge. The mean remained below the efficiency frontier, and differences widened after 2017. Higher performance in parts of Northwest and Northeast China contrasted with the relative lag of several central grain-producing provinces.

(2) The national network remained connected but became more selective. Density contracted and then partially recovered, while hierarchy increased, producing a differentiated multi-hub structure rather than uniform expansion.

(3) Centrality and block modeling revealed complementary structural positions. Key provinces acted as hubs or brokers, while the four blocks performed net-spillover, broker, bidirectional-spillover, and net-beneficiary functions. Within-block heterogeneity means that these roles should guide coordination modes rather than uniform provincial tasks.

(4) Persistence and reciprocity dominated network evolution. Similar urbanization and planting structures favored ties, while rural-income differences reflected socioeconomic complementarity. Shared partners generated neither additional closure nor expanding chains. External validation supported the broad network structure but only partly identified specific cooperation ties.

Governance should therefore prioritize the quality and durability of interprovincial coordination rather than network density alone. National standards and joint funding, broker-led multiyear coordination, and locally adapted implementation can be tested through monitored pilots before wider application.

Supplementary Materials: The following supporting information can be downloaded at: https://www.mdpi.com/article/10.3390/land15081491/s1, Figure S1 and Table S1 report threshold sensitivity; Figure S2 and Table S2 report weighted-centrality robustness; Figure S3 and Table S3 report the distance-excluded municipality-exclusion MRQAP test; Table S4 reports full province-level centrality results; Figure S4 and Table S5 report TERGM goodness-of-fit and model diagnostics; Table S6 reports the full-sample distance-excluded MRQAP estimates and model fit; Figure S5 reports the external validation against interprovincial green-technology patent collaboration.

Author Contributions: Conceptualization, Q.X. and Y.C. (Yinrong Chen); methodology, Q.X.; software, Q.X.; formal analysis, Q.X. and Y.C. (Yi Chen); data curation, Q.X. and Y.C. (Yi Chen); writing—original draft preparation, Q.X.; writing—review and editing, Y.C. (Yinrong Chen); visualization, Q.X.; supervision, Y.C. (Yinrong Chen). All authors have read and agreed to the published version of the manuscript.

Funding: This research was funded by the National Natural Science Foundation of China, grant number 42271270.

Data Availability Statement: The raw statistical data are publicly available in the China Statistical Yearbook, China Energy Statistical Yearbook, China Rural Statistical Yearbook, provincial statistical yearbooks, and provincial statistical bulletins. Administrative boundary data are available from the National Platform for Common Geospatial Information Services (https://www.tianditu.gov.cn/; accessed on 14 July 2026). The robustness outputs are provided in the Supplementary Materials. The processed matrices and analysis code are available from the corresponding author upon reasonable request. External-validation results are provided in the Supplementary Materials, while the analysis code is available from the corresponding author upon reasonable request. The interprovincial green-technology patent collaboration data were obtained from the China National Intellectual Property Administration (CNIPA).

Conflicts of Interest: The authors declare no conflicts of interest. The funder had no role in the design of the study; in the collection, analysis, or interpretation of data; in the writing of the manuscript; or in the decision to publish the results.

References

1. Meyfroidt, P.; de Bremond, A.; Ryan, C.M.; Archer, E.; Aspinall, R.; Chhabra, A.; Camara, G.; Corbera, E.; DeFries, R.; Diaz, S.; et al. Ten facts about land systems for sustainability. *Proc. Natl. Acad. Sci. USA* **2022**, *119*, e2109217118. [CrossRef] [PubMed]
2. Verburg, P.H.; Crossman, N.; Ellis, E.C.; Heinimann, A.; Hostert, P.; Mertz, O.; Nagendra, H.; Sikor, T.; Erb, K.-H.; Golubiewski, N.; et al. Land system science and sustainable development of the earth system: A global land project perspective. *Anthropocene* **2015**, *12*, 29–41. [CrossRef]
3. Foley, J.A.; Ramankutty, N.; Brauman, K.A.; Cassidy, E.S.; Gerber, J.S.; Johnston, M.; Mueller, N.D.; O'Connell, C.; Ray, D.K.; West, P.C.; et al. Solutions for a cultivated planet. *Nature* **2011**, *478*, 337–342. [CrossRef] [PubMed]
4. Lambin, E.F.; Meyfroidt, P. Global land use change, economic globalization, and the looming land scarcity. *Proc. Natl. Acad. Sci. USA* **2011**, *108*, 3465–3472. [CrossRef] [PubMed]
5. Liu, J.; Mooney, H.; Hull, V.; Davis, S.J.; Gaskell, J.; Hertel, T.; Lubchenco, J.; Seto, K.C.; Gleick, P.; Kremen, C.; et al. Systems integration for global sustainability. *Science* **2015**, *347*, 1258832. [CrossRef] [PubMed]
6. Meyfroidt, P.; Roy Chowdhury, R.; de Bremond, A.; Ellis, E.C.; Erb, K.-H.; Filatova, T.; Garrett, R.D.; Grove, J.M.; Heinimann, A.; Kuemmerle, T.; et al. Middle-range theories of land system change. *Glob. Environ. Change* **2018**, *53*, 52–67. [CrossRef]
7. Li, B.; Zhang, J.; Li, H. Spatio-temporal characteristics and influencing factor decomposition of agricultural carbon emissions in China. *China Popul. Resour. Environ.* **2011**, *21*, 80–86. (In Chinese)
8. Chen, L.; Xue, L.; Xue, Y. Spatio-temporal evolution characteristics of net carbon sink in China's agriculture. *J. Nat. Resour.* **2016**, *31*, 596–607. (In Chinese)
9. Smith, P.; Martino, D.; Cai, Z.; Gwary, D.; Janzen, H.; Kumar, P.; McCarl, B.; Ogle, S.; O'Mara, F.; Rice, C.; et al. Greenhouse gas mitigation in agriculture. *Philos. Trans. R. Soc. B Biol. Sci.* **2008**, *363*, 789–813. [CrossRef] [PubMed]
10. Roe, S.; Streck, C.; Beach, R.; Busch, J.; Chapman, M.; Daioglou, V.; Deppermann, A.; Doelman, J.; Emmet-Booth, J.; Engelmann, J.; et al. Land-based measures to mitigate climate change: Potential and feasibility by country. *Glob. Change Biol.* **2021**, *27*, 6025–6058. [CrossRef] [PubMed]
11. Smith, P.; Calvin, K.; Nkem, J.; Campbell, D.; Cherubini, F.; Grassi, G.; Korotkov, V.; Le Hoang, A.; Lwasa, S.; McElwee, P.; et al. Which practices co-deliver food security, climate change mitigation and adaptation, and combat land degradation and desertification? *Glob. Change Biol.* **2020**, *26*, 1532–1575. [CrossRef] [PubMed]
12. Tilman, D.; Balzer, C.; Hill, J.; Befort, B.L. Global food demand and the sustainable intensification of agriculture. *Proc. Natl. Acad. Sci. USA* **2011**, *108*, 20260–20264. [CrossRef] [PubMed]
13. Burney, J.A.; Davis, S.J.; Lobell, D.B. Greenhouse gas mitigation by agricultural intensification. *Proc. Natl. Acad. Sci. USA* **2010**, *107*, 12052–12057. [CrossRef] [PubMed]
14. Searchinger, T.D.; Wirsenius, S.; Beringer, T.; Dumas, P. Assessing the efficiency of changes in land use for mitigating climate change. *Nature* **2018**, *564*, 249–253. [CrossRef] [PubMed]
15. West, P.C.; Gerber, J.S.; Engstrom, P.M.; Mueller, N.D.; Brauman, K.A.; Carlson, K.M.; Cassidy, E.S.; Johnston, M.; MacDonald, G.K.; Ray, D.K.; et al. Leverage points for improving global food security and the environment. *Science* **2014**, *345*, 325–328. [CrossRef] [PubMed]
16. Springmann, M.; Clark, M.; Mason-D'Croz, D.; Wiebe, K.; Bodirsky, B.L.; Lassaletta, L.; de Vries, W.; Vermeulen, S.J.; Herrero, M.; Carlson, K.M.; et al. Options for keeping the food system within environmental limits. *Nature* **2018**, *562*, 519–525. [CrossRef] [PubMed]
17. Clark, M.A.; Domingo, N.G.G.; Colgan, K.; Thakrar, S.K.; Tilman, D.; Lynch, J.; Azevedo, I.L.; Hill, J.D. Global food system emissions could preclude achieving the 1.5 and 2 degrees C climate change targets. *Science* **2020**, *370*, 705–708. [CrossRef] [PubMed]
18. Tone, K. A slacks-based measure of super-efficiency in data envelopment analysis. *Eur. J. Oper. Res.* **2002**, *143*, 32–41. [CrossRef]
19. Pastor, J.T.; Lovell, C.A.K. A global Malmquist productivity index. *Econ. Lett.* **2005**, *88*, 266–271. [CrossRef]
20. Wu, H.; Sipilainen, T.; He, Y.; Huang, H.; Luo, L.; Chen, W.; Meng, Y. Performance of cropland low-carbon use in China: Measurement, spatiotemporal characteristics, and driving factors. *Sci. Total Environ.* **2021**, *800*, 149552. [CrossRef] [PubMed]
21. Cheng, C.; Li, J.; Qiu, Y.; Gao, C.; Gao, Q. Evaluating the spatiotemporal characteristics of agricultural eco-efficiency alongside China's carbon neutrality targets. *Int. J. Environ. Res. Public Health* **2022**, *19*, 15478. [CrossRef] [PubMed]
22. Yang, B.; Wang, Z.; Zou, L.; Zou, L.; Zhang, H. Exploring the eco-efficiency of cultivated land utilization and its influencing factors in China's Yangtze River Economic Belt, 2001–2018. *J. Environ. Manag.* **2021**, *294*, 112939. [CrossRef] [PubMed]
23. Yin, Y.; Hou, X.; Liu, J.; Zhou, X.; Zhang, D. Detection and attribution of changes in cultivated land use ecological efficiency: A case study on Yangtze River Economic Belt, China. *Ecol. Indic.* **2022**, *137*, 108753. [CrossRef]

24. Hou, X.; Liu, J.; Zhang, D.; Zhao, M.; Xia, C. Impact of urbanization on the eco-efficiency of cultivated land utilization: A case study on the Yangtze River Economic Belt, China. *J. Clean. Prod.* **2019**, *238*, 117916. [CrossRef]
25. Fan, Y.; Ning, W.; Liang, X.; Wang, L.; Lv, L.; Li, Y.; Wang, J. Spatial-temporal characteristics and influencing factors of eco-efficiency of cultivated land use in the Yangtze River Delta Region. *Land* **2024**, *13*, 219. [CrossRef]
26. Kohler, J.; Geels, F.W.; Kern, F.; Markard, J.; Onsongo, E.; Wieczorek, A.; Alkemade, F.; Avelino, F.; Bergek, A.; Boons, F.; et al. An agenda for sustainability transitions research: State of the art and future directions. *Environ. Innov. Soc. Transit.* **2019**, *31*, 1–32. [CrossRef]
27. Geels, F.W. The multi-level perspective on sustainability transitions: Responses to seven criticisms. *Environ. Innov. Soc. Transit.* **2011**, *1*, 24–40. [CrossRef]
28. Pretty, J.; Benton, T.G.; Bharucha, Z.P.; Dicks, L.V.; Flora, C.B.; Godfray, H.C.J.; Goulson, D.; Hartley, S.; Lampkin, N.; Morris, C.; et al. Global assessment of agricultural system redesign for sustainable intensification. *Nat. Sustain.* **2018**, *1*, 441–446. [CrossRef]
29. Liu, J.; Hull, V.; Batistella, M.; DeFries, R.; Dietz, T.; Fu, F.; Hertel, T.W.; Izaurralde, R.C.; Lambin, E.F.; Li, S.; et al. Framing sustainability in a telecoupled world. *Ecol. Soc.* **2013**, *18*, 26. [CrossRef]
30. Khan, J. What role for network governance in urban low carbon transitions? *J. Clean. Prod.* **2013**, *50*, 133–139. [CrossRef]
31. Yang, J.; Luo, P. Study on the spatial correlation network structure of agricultural carbon emission efficiency in China. *Electron. Res. Arch.* **2023**, *31*, 7256–7283. [CrossRef]
32. Xu, W.; Chen, B. Spatial association network structure of agricultural carbon emission efficiency in Chinese cities and its driving factors. *Sci. Rep.* **2024**, *14*, 31810. [CrossRef] [PubMed]
33. He, W.; Wang, F.; Feng, N.; Cheng, J. Research on the characteristics and influencing factors of the spatial correlation network of cultivated land utilization ecological efficiency in the upper reaches of the Yangtze River, China. *PLoS ONE* **2024**, *19*, e0297933. [CrossRef] [PubMed]
34. Zhi, Y.; Zhang, F.; Wang, H.; Qin, T.; Tong, J.; Wang, T.; Wang, Z.; Kang, J.; Fang, Z. Agricultural water use efficiency: Is there any spatial correlation between different regions? *Land* **2022**, *11*, 77. [CrossRef]
35. Yang, G.; Gong, G.; Gui, Q. Exploring the spatial network structure of agricultural water use efficiency in China: A social network perspective. *Sustainability* **2022**, *14*, 2668. [CrossRef]
36. Fang, F.; Zhao, J.; Di, J.; Zhang, L. Spatial correlations and driving mechanisms of low-carbon agricultural development in China. *Front. Environ. Sci.* **2022**, *10*, 1014652. [CrossRef]
37. Zhou, Z.; Duan, J.; Geng, S.; Li, R. Spatial network and driving factors of agricultural green total factor productivity in China. *Energies* **2023**, *16*, 5380. [CrossRef]
38. Xu, Y.; Wang, D.; Zhang, Y. Analysis of the spatial association network of agricultural water use efficiency and its driving factors in China. *Front. Environ. Sci.* **2026**, *13*, 1730331. [CrossRef]
39. Zhang, Y.; Sun, Y.; Liang, H. Spatial linkage network patterns and driving mechanisms of urban land use efficiency: Evidence from Yangtze River Delta urban agglomeration, China. *Appl. Geogr.* **2026**, *186*, 103867. [CrossRef]
40. Hanneke, S.; Fu, W.; Xing, E.P. Discrete temporal models of social networks. *Electron. J. Stat.* **2010**, *4*, 585–605. [CrossRef]
41. Leifeld, P.; Cranmer, S.J.; Desmarais, B.A. Temporal exponential random graph models with btergm: Estimation and bootstrap confidence intervals. *J. Stat. Softw.* **2018**, *83*, 1–36. [CrossRef]
42. Krivitsky, P.N.; Handcock, M.S. A separable model for dynamic networks. *J. R. Stat. Soc. Ser. B Stat. Methodol.* **2014**, *76*, 29–46. [CrossRef] [PubMed]
43. Snijders, T.A.B.; van de Bunt, G.G.; Steglich, C.E.G. Introduction to stochastic actor-based models for network dynamics. *Soc. Netw.* **2010**, *32*, 44–60. [CrossRef]
44. Butts, C.T. A relational event framework for social action. *Sociol. Methodol.* **2008**, *38*, 155–200. [CrossRef]
45. Sewell, D.K.; Chen, Y. Latent space models for dynamic networks. *J. Am. Stat. Assoc.* **2015**, *110*, 1646–1657. [CrossRef]
46. Leifeld, P.; Cranmer, S.J. A theoretical and empirical comparison of the temporal exponential random graph model and the stochastic actor-oriented model. *Netw. Sci.* **2019**, *7*, 20–51. [CrossRef]
47. Fritz, C.; Lebacher, M.; Kauermann, G. Tempus volat, hora fugit: A survey of tie-oriented dynamic network models in discrete and continuous time. *Stat. Neerl.* **2020**, *74*, 275–299. [CrossRef]
48. Ke, N.; Lu, X.; Kuang, B.; Han, J. Regional differences and influencing factors of green low-carbon utilization of cultivated land in China under carbon neutrality target. *China Land Sci.* **2021**, *35*, 67–76. (In Chinese)
49. Ding, Y.; Guo, Q.; Qin, M. Spatio-temporal evolution and influencing factors of green land use efficiency in resource-based cities of the Yellow River Basin. *Trans. Chin. Soc. Agric. Eng.* **2021**, *37*, 250–259. (In Chinese)
50. Zhu, Q.; Chen, Y.; Hu, W.; Mei, Y. Spatio-temporal patterns of coupling coordination between intensive land use and regional eco-efficiency in China. *Trans. Chin. Soc. Agric. Eng.* **2020**, *36*, 234–243. (In Chinese)
51. Lan, Z.; Chen, X.; Liu, Y.; Wu, H.; He, W.; Li, W. Assessment of provincial low-carbon economic performance from a resilience development perspective and impact of regional network governance. *Econ. Geogr.* **2024**, *44*, 42–51. (In Chinese)

52. Liu, M.; Chen, Y.; Wang, J.; Chen, K.; Chen, Y. Spatial correlation network and driving factors of carbon emission efficiency in land use in China. *Resour. Sci.* **2024**, *46*, 2462–2476. (In Chinese) [CrossRef]
53. Ji, X.; Zhang, Y. Spatial correlation network structure and drivers of carbon emission efficiency in planting industry of the Yangtze River Economic Belt. *J. Nat. Resour.* **2023**, *38*, 675–693. (In Chinese) [CrossRef]
54. Shao, X.; Yao, Y. Spatial network characteristics and influence mechanisms of the urban agglomeration in the middle reaches of the Yangtze River. *Urban Probl.* **2019**, *10*, 15–26. (In Chinese)
55. Zhou, D.; Li, S.; Li, H.; Ding, Q.; Pan, S.; Wang, Y. Green use efficiency of cultivated land at the municipal level in China from a telecoupling perspective: Spatial association network characteristics and management strategies. *China Land Sci.* **2025**, *39*, 113–126. (In Chinese) [CrossRef]
56. Zhang, L.; Sun, P. Spatial correlation network and influencing factors of urban ecological resilience in the Yangtze River Delta. *Resour. Environ. Yangtze Basin* **2025**, *34*, 2781–2794. (In Chinese) [CrossRef]
57. Dekker, D.; Krackhardt, D.; Snijders, T.A.B. Sensitivity of MRQAP tests to collinearity and autocorrelation conditions. *Psychometrika* **2007**, *72*, 563–581. [CrossRef] [PubMed]
58. Krackhardt, D. QAP partialling as a test of spuriousness. *Soc. Netw.* **1987**, *9*, 171–186. [CrossRef]
59. Klerkx, L.; Proctor, A. Beyond fragmentation and disconnect: Networks for knowledge exchange in the English land management advisory system. *Land Use Policy* **2013**, *30*, 13–24. [CrossRef]
60. Simpson, H.C.; de Loë, R.C. The Agricultural Community as a Social Network in a Collaborative, Multi-Stakeholder Problem-Solving Process. *Water* **2017**, *9*, 750. [CrossRef]
61. Hermans, F.; Sartas, M.; van Schagen, B.; van Asten, P.; Schut, M. Social network analysis of multi-stakeholder platforms in agricultural research for development: Opportunities and constraints for innovation and scaling. *PLoS ONE* **2017**, *12*, e0169634. [CrossRef] [PubMed]

Disclaimer/Publisher's Note: The statements, opinions and data contained in all publications are solely those of the individual author(s) and contributor(s) and not of MDPI and/or the editor(s). MDPI and/or the editor(s) disclaim responsibility for any injury to people or property resulting from any ideas, methods, instructions or products referred to in the content.